PERGAMON

Journal of Structural Geology 23 (2001) 1345–1357

JOURNAL OF STRUCTURAL GEOLOGY

www.elsevier.com/locate/jstrugeo

A pseudotachylyte geothermometer

Kieran D. O'Hara*

Department of Geological Sciences, University of Kentucky, Lexington, KY 40502, USA

Received 7 February 2000; accepted 12 December 2000

Abstract

Pseudotachylytes invariably contain a conspicuous concentration of clasts and lithic fragments in their matrices, which reflect brittle wear processes during frictional melting. The ratio of clasts to matrix is interpreted as the ratio of wear to melt (*W/M*) and measurements of this ratio show a range of 0.1–0.7. Based on models of melting and wear processes it is shown that the ratio *W/M* is independent of fault displacement, stress, fault area and mineralogy. Thermodynamic considerations indicate that *W/M* corresponds to the thermodynamic efficiency of the conversion of work to heat and is defined as $w/q = (T_{high} - T_{low})/T_{high}$ where T_{high} refers to the melt temperature and T_{low} is the ambient country rock temperature. This provides a simple new technique for estimating the ambient crustal temperature T_{crust}, in degrees Kelvin

$$T_{crust} = (1 - W/M)T_{melt.}$$

Assuming a reasonable value for the temperature of the melt, estimates of country rock temperatures T_{crust} for pseudotachylytes from four different localities in the USA indicate a range of 123–387°C. Eclogite-facies pseudotachylytes from western Norway yield a mean country rock temperature of 658°C, in good agreement with independent Fe–Mg exchange geothermometry. This new geothermometer appears to be applicable throughout the entire crust and may provide a better understanding of melting and wear processes during seismic faulting. © 2001 Elsevier Science Ltd. All rights reserved.

1. Introduction

There is substantial interest in pseudotachylytes as products of frictional melting because they represent one of the few indicators of seismic activity in the geologic record (Sibson, 1975; Swanson, 1992). Current rheological models of the continental crust (Snoke and Tullis, 1998) indicate that frictional melting should be most common in the brittle upper crust, but that frictional melting may also occur below the brittle-plastic transition, either due to downward propagation of a brittle rupture front (e.g. Scholz, 1990), or due to heterogeneous localized high stress regions (Sibson, 1980) or by development of an instability in the deeper ductile crust (Hobbs et al., 1986). More recent discoveries of ultra deep pseudotachylyte developed under eclogite conditions (Austrheim and Boundy, 1994) and theoretical considerations that indicate frictional melting can occur during deep earthquakes (Kanamori et al., 1998) suggest frictional melting can occur throughout the entire lithosphere. Further testing, refinement, and calibration of these models is desirable and could be undertaken if a widely applicable geothermometer for frictionally melted rocks existed. Moreover, such a geothermometer would allow examination of the depth relationship between seismicity and frictional melting throughout the crust and deeper levels. Here, a simple geothermometer, applicable to most fault-generated pseudotachylytes, is outlined and it is used to estimate the depth of melting in the crust for pseudotachylytes from five different localities.

2. Clast/matrix ratios in pseudotachylytes

Pseudotachylytes invariably contain products of frictional wear (lithic fragments, clasts, gouge, etc.) so that, in addition to information on frictional heating, they also contain information on the nature of fracture and communition processes during seismic rupture. Frictional melting and brittle fracturing during coseismic slip are closely related processes and several workers have pointed to a close association between pseudotachylytes and cataclastic rocks (e.g. Magloughlin, 1992). Frictional heating and melting likely initiate at asperity contacts (Logan and Teufel, 1986; Spray, 1995). These asperities then either undergo total (or partial) melting or shear off and become imbedded in the melt. On cooling, the rock, therefore, preserves a record of the

* Fax: +1-859-323-1938.
E-mail address: geokoh@pop.uky.edu (K.D. O'Hara).

0191-8141/01/$ - see front matter © 2001 Elsevier Science Ltd. All rights reserved.
PII: S0191-8141(01)00008-6

relative importance of thermal and mechanical processes during seismic slip (e.g. Fig. 1a).

The factors affecting frictional melting are many, including thermal conductivity and melting temperature of asperities, heat generation rate, shear stress and the presence (or absence) of water (Spray, 1992). Similarly, brittle wear processes also depend on several geologic variables such as yield strength of asperities, fault displacement, surface roughness, depth of faulting and lithology (e.g. Scholz, 1987; Power et al., 1988). The concentration of clasts in the pseudotachylyte matrix should, therefore, be expected to be highly variable. Contrary to expectation, the clast/matrix ratio (*W*/*M*) ratio observed in five geologically unrelated fault-generated pseudotachylytes display a limited range of 0.1–0.7 (Table 1; Fig. 2). These localities have been described in detail elsewhere and only a brief description of the geologic setting of each locality is provided below.

3. Geologic settings

3.1. Cascade Mountains, Washington

The pseudotachylytes from the Cascade Mountains formed in several lithologies, including pelitic schist and tonalite of the Nason terrane in post middle Cretaceous to Tertiary time (Magloughlin, 1989). Pseudotachylytes are developed parallel and within a regional foliation and also along fault generation surfaces. The samples examined in this study are developed in medium grained (1–2 mm) foliated plagioclase biotite–hornblende gneiss of the Mount Stuart batholith and are texturally associated with cataclasites, which appear to be a precursor to melting (Magloughlin, 1992). Evidence for melting includes microlites, melt droplets of sulfide, flow structures, the presence of glass, vesicles and dendritic microphenocrysts (Magloughlin, 1998).

3.2. Fort Foster, Maine

The pseudotachylytes developed at Fort Foster are well exposed in a Late Paleozoic right-lateral brittle zone in the northern Appalachians of coastal Maine. The samples examined in this study are from Fort Foster State park and are hosted by fine-grained (<0.1 mm) mylonitic plagioclase–hornblende–biotite-bearing metasedimentary rocks (Swanson, 1988). Microprobe analyses of the matrix indicate a similar composition to the host rock (O'Hara and Sharp, 2001) suggesting near total melting. Fault displacements are in the range of tens of centimeters. Injection veins 1–2 cm in length at a high angle to fault surfaces are common and in thin section they commonly exhibit folded flow structures (Fig. 1b). Ductile fabrics overprint some injection veins suggesting melting occurred close to the brittle-plastic transition (Swanson, 1988). Clasts, which are commonly rounded and embayed, are dominated by mylonitic quartz and lithic fragments.

3.3. South Mountain, Arizona

The pseudotachylytes at South Mountain occur in Tertiary cataclastic and mylonitic granite, alaskite and biotite–granodiorite in an extensional shear zone related to core complex formation during the middle Tertiary (Reynolds and Lister, 1987). In thin section, the pseudotachylytes are locally overprinted by mylonitic textures (Fig. 1c), indicating some formed below the brittle-plastic transition in the crust (Goodwin et al., 1998). The textures in the host rocks suggest mylonitization occurred under lower greenschist facies conditions. Injection veins off the main fault surface are common and usually show internal flow folding in thin section. Melting in some cases is thought to have initiated along biotite-bearing micro shears in the host rock (Goodwin and Ferranti, 1994). The samples examined in this study are from Dobbins' Lookout and Telegraph Pass Trail (Reynolds and Lister, 1987) and do not show mylonitic overprints. The clasts in the pseudotachylyte matrix are dominantly quartz and lithic fragments that are commonly rounded and embayed. Some contain long tails suggesting partial melting of the clasts. The presence of glass confirms a melt origin (Goodwin et al., 1998).

3.4. Homestake shear zone, Colorado

Pseudotachylytes from the Homestake shear zone occur in a multiply reactivated basement shear zone developed in Middle Proterozoic coarse-grained gneisses and biotite–sillimanite granites (Allen, 1994). Embayments into the wall rock along melt boundaries commonly correspond to biotite grains, suggesting preferential melting of biotite (Fig. 1d). Microprobe analyses also suggest preferential melting of biotite and alkali feldspar (O'Hara and Sharp, 2001). The presence of micron-sized dendritic crystals of magnetite in the pseudotachylyte matrix confirms a melt origin. The presence of acicular mullite, an alumino-silicate associated with contact metamorphism near volcanic rocks, in the pseudotachylyte matrix indicates high melting temperatures (Moecher et al., 1999).

3.5. Bergen Arcs, western Norway

Ultra deep (>60 km) pseudotachylytes from western Norway are hosted in meta-anorthosite and contain an eclogite facies assemblage of plagioclase–garnet–omphacite–kyanite (Austrheim and Boundy, 1994). The pseudotachylytes are thought to have formed as a result of volume changes related to eclogitization during Caledonian-aged subduction. Fault-related pseudotachylytes are 1–5 cm thick and can be traced for >10 m. Small euhedral garnets and acicular kyanite are common in the pseudotachylyte matrix (Boundy and Austrheim, 1998). Temperature and pressure estimates of the host

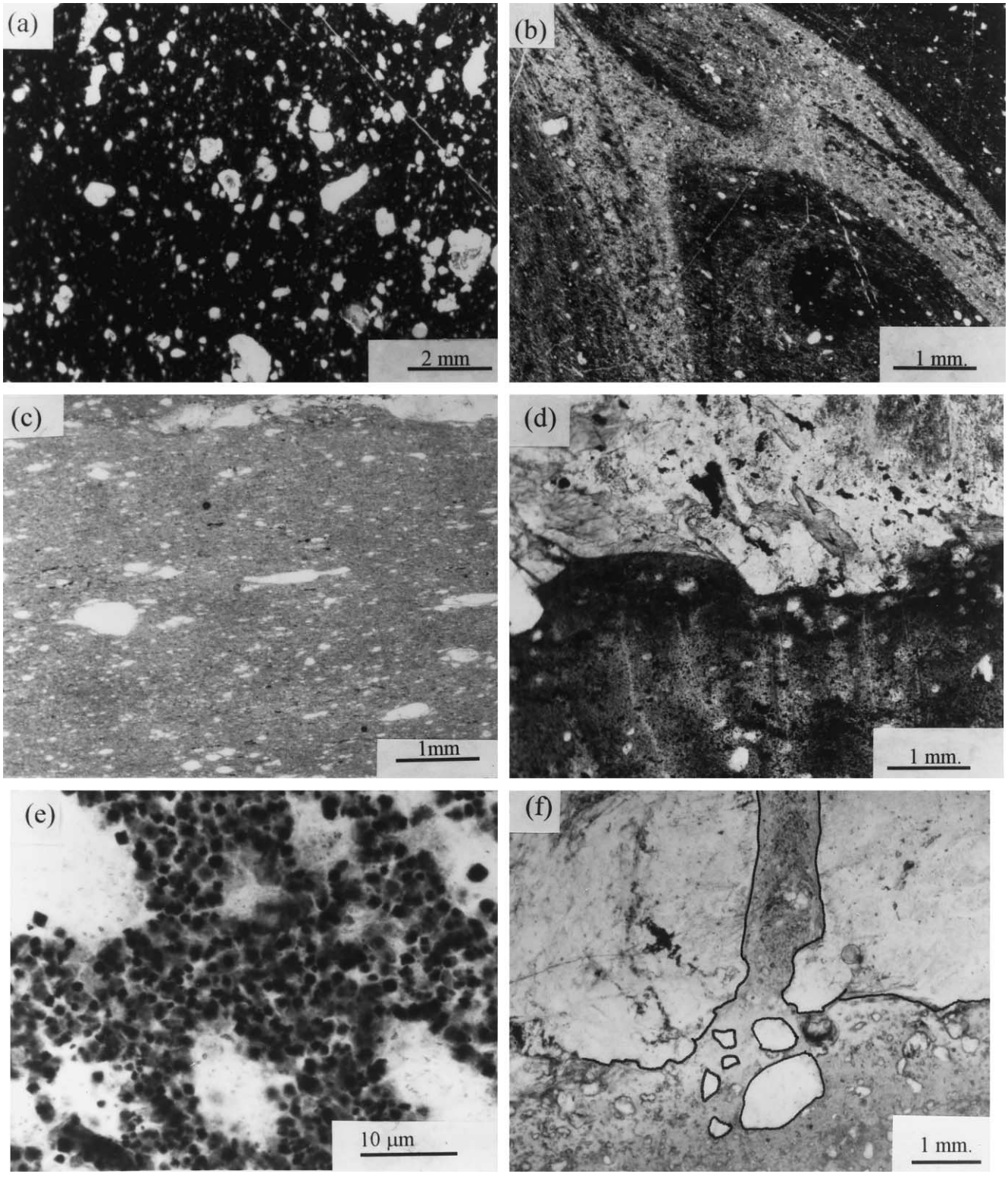

Fig. 1. Pseudotachylyte photomicrographs. (a) Clasts in pseudotachylyte matrix that represent material produced during brittle wear processes. From Homestake shear zone, PPL. (b) Flow fold in injection vein from Fort Foster locality. These veins tend to have a lower concentration of clast material compared with fault generation surfaces. (c) Mylonitic foliation overprinting pseudotachylyte from South Mountain. Sample courtesy of J. Reynolds. (d) Embayments of the melt into the country rock correspond to biotite grains, suggesting biotite melting. From Homestake shear zone, XP. (e) Quartz clasts under high power (1000 ×) oil immersion objective. These clasts are rarely less than 5 μm in diameter. Euhedral dark grains are magnetite 2 μm in diameter and are easily resolvable at this magnification. Homestake shear zone, PPL. (f) Clasts concentrated at mouth of an injection vein, suggesting a bottleneck effect, resulting in lower clast concentrations in the vein, PPL.

Table 1
Pseudotachylyte localities, wear/melt ratios (*W/M*) and temperature estimates

Locality and sample #	Clast type[a]	*W/M*[b] (s.d.), *n*	T_{melt} (°C)[c]	T_{crust} (°C)[d]	Metamorphic grade of host
Homestake zone					
41.15 (fault)	Q, LF	0.64 (0.015), 3	927	159	Sillimanite
41.9 (fault)	Q, LF	0.67 (0.07), 2	927	123	Sillimanite
41.6 (fault)	Q, LF	0.66 (0.007), 2	927	135	Sillimanite
41.5 (fault)	Q, LF	0.66 (0.07), 4	927	135	Sillimanite
22.3 (fault)	Q,LF	0.53 (0.05), 3	927	291	Sillimanite
32.5 (fault)	Q,LF	0.48 (0.06), 3	927	351	Sillimanite
14.5 (fault)	Q,LF	0.47 (0.04), 4	927	363	Sillimanite
22.4 (vein)	Q, LF	0.29 (0.05), 3	–	–	Sillimanite
Fort Foster fault					
11.Rye.95 (fault)	Q, F	0.71 (0.08), 4	927	75	Greenschist
80.Rye.99 (fault)	Q,	0.45 (0.01), 2	927	387	Amphibolite
210.Rye.99 (vein)	Q	0.46 (0.07), 2	–	–	Amphibolite
South Mt.					
SM1C.AZ (fault)	Q	0.66 (0.07), 2	927	135	Greenschist
SM2.AZ (vein)	Q	0.27 (0.0), 2	–	–	Greenschist
Mt. Stuart tonalite					
20.WA.95 (fault)	Q, LF	0.57 (0.08), 2	927	243	Amphibolite
30.WA.95 (fault)	Q, LF	0.53 (0.06), 2	927	291	Amphibolite
Western Norway					
Isdahl (fault)	Q	0.15, 1	927 (800)[e]	747 (639)	Eclogite
ABE 28 (fault)	Q	0.12,1	927 (800)	783 (671)	Eclogite
ABE 32 (fault)	Q	0.09,1	927 (800)	723 (703)	Eclogite
HA25 (fault)	Q	0.17,1	927 (800)	819 (618)	Eclogite

[a] Q = quartz, F = feldspar, LF = lithic fragments.
[b] 200 point counts per sample; (s.d.) = 2σ standard deviation; n = number of repeat measurements.
[c] Assumed melt temperature.
[d] T_{crust} (K) = $(1 - W/M)T_{melt}$ (K).
[e] Based on Fe–Mg geothermometry.

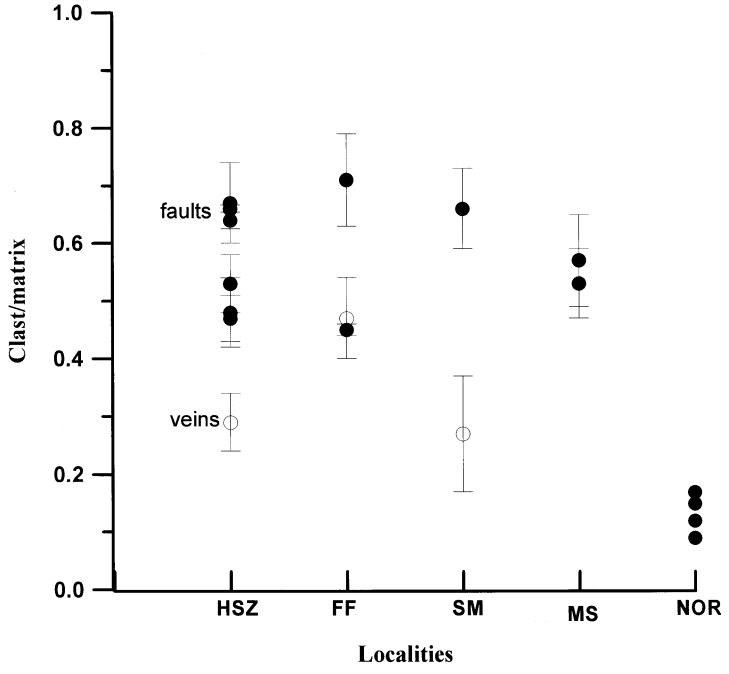

Fig. 2. Plot of *W/M* ratios for pseudotachylyte localities based on data in Table 1. Solid circles represent pseudotachylytes on faults and open circles represent injection vein pseudotachylytes. HSZ—Homestake shear zone; FF—Fort Foster fault; SM—South Mountain; MS—Mount Stuart batholith. NOR—western Norway. Error bars represent 2σ.

rock are 670°C and >15 kb and Fe–Mg exchange between garnet and pyroxene indicate minimum temperatures of 790–920°C for the melt phase (Austrheim et al., 1996).

4. Methods

Clast/matrix ratios were measured on thin (30–μm) sections from the five localities described above by point counting 200 points per section at 100–μm intervals under the optical microscope using a 100× oil immersion objective lens, giving a total magnification of 1000×. This objective lens has a resolution of 2 μm, which on the basis of back-scattered electron (BSE) imagery, is smaller than the smallest fragments in these rocks. Under the optical microscope, fragments smaller than 5 μm are rarely observed (Fig. 1e). The optical microscope allows entire thin sections to be point counted, providing a more representative measure of the clast concentration compared with BSE or transmission electron microscopy (TEM) imagery.

Preferential melting of the fine-grained fraction of clasts likely occurs during frictional melting, thereby altering the grain-size distribution (Shimamoto and Nagahama, 1992; Ray, 1999; Tsutsumi, 1999). Studies of the volume of clast material in pseudotachylytes as a function of clast size suggest an approximate log normal distribution, with the mean clast volume corresponding to clast sizes in the interval 30–100 μm (Fig. 7 in Ray (1999)). This broadly corresponds to point counting on the thin section scale with 100 μm stepping intervals. High power techniques such as BSE or TEM will under estimate the clast/matrix ratio in the size interval of about 1–10 μm, and this is attributed to preferential melting of this size fraction (Ray, 1999). At scales larger than the thin section the clast/matrix ratio is commonly either under or over represented (Fig. 7 in Ray (1999)).

The host rocks are all quartzo-feldspathic in composition. The composition of clasts was identified under both optical and BSE microscopy and is dominated by quartz, followed by host rock lithic fragments (Table 1). Quartz and lithic fragments are recognized under cross-polarized light by their higher birefringence compared with the matrix, which is usually dark. Under plane polarized light, clasts are colorless and have a distinct relief compared with the matrix. Repeated measurements on the same thin section indicate that the coefficient of variation (σ/mean × 100) on clast/matrix ratios is <10% (Table 1).

Measurements of clast/matrix ratios were also made on injection veins (as opposed to fault generation surfaces) from three of the localities described above (Table 1; Fig. 2). The clast/matrix ratio appears to be lower in the injection vein pseudotachylytes compared with the fault surfaces, suggesting some process has modified this ratio during injection. It has been suggested that the lower clast/matrix ratio in injection veins is caused by a filtering effect by narrow openings in the cataclastically deformed host rock such that larger clasts are screened out (Ray, 1999). Fig. 1f shows such a 'bottleneck' at the mouth of an injection vein where clasts are concentrated. This suggests that fault generation surfaces provide a more reliable estimate of the original clast/matrix ratio.

It has been shown, on the basis of the self-similar clast size distribution in both natural pseudotachylytes (Shimamoto and Nagahama, 1992) and artificial frictional melts (Tsutsumi, 1999) that the matrix of pseudotachylytes represents a melt phase rather than the product of ultra-fine communition. The clast/matrix ratio is, therefore, interpreted as the frictional wear/melt ratio and is henceforth referred to as *W/M*.

The *W/M* ratio on fault generation surfaces from the five localities in this study has a range from 0.1 (±0.00) to 0.7 (±0.08) (Table 1; Fig. 2). A review of published descriptions of other pseudotachylyte localities indicates a similar range. Shimamoto and Nagahama (1992) report a *W/M* ratio of 0.66 for pseudotachylytes from the Musgrave Range, central Australia. Spray (1993) reported the clast/total volume ratios for eight unrelated natural pseudotachylytes (including two impact related melts and two artificial pseudotachylytes), which when recalculated as *W/M* ratios, give a lower mean value of 0.18 ± 0.06 ($n = 10$). For pseudotachylytes from NW Scotland, Maddock (1992) reported a mean *W/M* ratio of 0.36 ± 0.06 ($n = 5$) based on point counting. Techmer et al. (1992) report an average clast volume of about 30% corresponding to a *W/M* ratio of 0.42 for pseudotachylytes from the Italian Alps. The range of the estimates from these five additional studies is 0.18–0.66. The total range in the *W/M* ratios from all localities, including the five localities of this study, is, therefore, 0.1–0.7.

In the cases above, a substantial bias may be present because of the different methods of measurement at different magnifications. As noted above, the *W/M* ratio, when measured on the thin-section scale, corresponds to the mean clast volume (Ray, 1999) and is thought to be more representative than measurements at either higher or lower scales. A distinction between injection veins and fault generation surfaces is not always made in the above studies, suggesting the lower end of the range could reflect modification of *W/M* during injection. Nevertheless, given the large number of variables that are likely to affect this ratio, the observed range is limited. In principle, the wear/melt ratio could range from zero (for a pure melt) to infinity for a melt-free cataclasite. Models for wear processes and frictional melting processes are examined below with a view to gaining insight into the nature of this parameter.

5. Models of wear and melt processes

5.1. Volume of frictional wear

Mechanical wear processes in rock friction experiments

display an initially high (transient) wear phase, followed by a slower steady-state wear phase (Power et al., 1988; Wang and Scholz, 1994). Based on models and experiments on wear processes in metals (Archard, 1953), an expression for the volume of steady state wear (W) in rocks is given by (Scholz, 1987):

$$W = Ak\sigma x/3h \tag{1}$$

where A is the fault area, k is the wear coefficient, which includes the probability that an asperity is sheared off per unit slip distance, h is a hardness property that is also a measure of the strength of the asperities, x is displacement and σ is the normal stress across the fault. This model predicts that wear volume is proportional to normal load and inversely proportional to the strength of the asperities. The model also predicts a linear relationship between displacement and clast volume. Although this is consistent with observations on natural faults (Scholz, 1987), such a linear relationship may not persist for long if gouge particles separate the fault surfaces from contact with each other or if wear occurs under transient conditions. On the other hand, if fault roughness scales with displacement, then the wear volume and thickness will increase with displacement (Scholz, 1987; Power et al., 1988).

Transient wear represents a 'running in' or pre-conditioning of the fault surfaces before settling down to a lower steady-state wear rate. Under transient conditions, the volume of wear material in experimental rock studies has been successfully modeled using the following expression (Power et al., 1988; see also Wang and Scholz, 1994):

$$W = v_0[1 - \exp(-nx)] \tag{2}$$

where v_0 is the initial volume by which the fault surface departs from a flat surface. This volume is defined as $v_0 = 2Ar$, where A is the area of the fault and r is the initial roughness. Initial roughness is defined as an average distance by which the fault surface departs from a flat surface. In Eq. (2), n is a constant that enfolds several variables including, but not limited to, asperity hardness, stress, temperature, fluid pressure (Power et al., 1988). This equation and experimental data indicate that the transient wear rate is initially exponential but levels off rapidly so that the wear volume approaches the constant v_0 after a small displacement. A physical interpretation for this process involves shearing off of asperities during the initial high wear production phase, when fault roughness is high, followed by riding of asperities over each other as the surfaces become smooth (Wang and Scholz, 1994).

5.2. Volume of frictional melt

If all the work is dissipated as frictional heat, the steady state volume of melt (M) produced during slip is given by (e.g. Sibson, 1975):

$$M = A\tau x/q \tag{3}$$

where τ is the shear stress across the fault and q is the amount of heat required to melt the source rock. This model predicts a linear relationship between melt volume and displacement. If, as has been suggested (e.g. McKenzie and Brune, 1972), the presence of melt lowers the shear stress on the fault, thereby reducing the amount of frictional heat, then the melt production will be self limiting. For simplicity it is assumed here that shear stress decreases linearly with the melt fraction, M/V, where V is fault volume, so that:

$$\tau = \tau_0(1 - M/V) \tag{4}$$

where τ_0 is the initial shear stress. As the melt volume, M, approaches the volume of the fault, V, the shear stress goes to zero. Substituting Eq. (4) into Eq. (3) and differentiating gives the melting rate:

$$\mathrm{d}M/\mathrm{d}x = A\tau_0(1 - M/V)/q. \tag{5}$$

The solution to this differential equation is:

$$M = V[1 - \exp(-A\tau_0 x/qV)]. \tag{6}$$

This equation indicates the melt volume rapidly approaches the fault volume, V, after a small displacement and then remains constant. Once the shear stress goes to zero, the fault dissipates no more frictional energy. If the rupture continues, however, the fault could expend work by radiation of seismic energy, but evidence cited below suggests this energy is small compared with the total energy.

5.3. Steady state wear/melt ratios

The ratio of steady state wear volume, W, to frictional melt volume, M, can be calculated using the equations presented above. The ratio of Eqs. (1) and (3) is:

$$W/M = kq/3h\mu \tag{7}$$

where τ is replaced by $\mu\sigma$ in Eq. (3), and μ is the coefficient of friction. This expression is independent of displacement, fault area, and stress. The coefficient of friction has a restricted range of 0.6–0.85 for most rocks (Byerlee's law) and is independent of temperature under brittle conditions (Scholz, 1990). Also, the ratio of thermal energy needed to melt asperities and the strength of the asperities q/h appears to be constant for most silicate minerals, as indicated below.

Fig. 3 shows a plot of thermal energy required for melting versus yield strength for several common rock-forming silicates, based on data in Table 2. The thermal energy is given by $q = C_p\Delta T + H_f$, where C_p is the heat capacity at constant pressure, which is itself a function of temperature, ΔT is the interval of heating from the ambient temperature of the country rock (chosen to be 200°C) to the melting point of the mineral in question. H_f is the latent heat of fusion. Because of an approximate linear relationship between temperature and C_p (Robie et al., 1978), a value for C_p was chosen at a temperature approximately midway in the heating interval (Table 2).

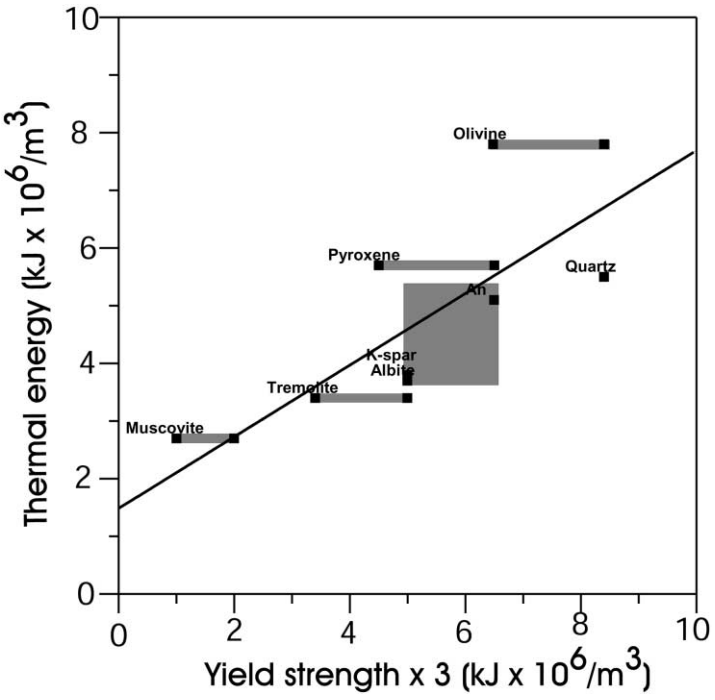

Fig. 3. Plot of thermal energy needed to melt the common rock-forming silicate minerals versus three times yield strength, based on the last two columns in Table 2. The best fit line has a slope of 0.62 ($r^2 = 0.61$) and represents $q/3h$. It is suggested that $q/3h$ in Eq. (7) is, therefore, independent of mineralogy.

A strong positive correlation exists between the thermal energy necessary to heat and melt a mineral and the yield strength of that mineral, such that the ratio q/h is roughly constant (Fig. 3). A positive correlation between the melting temperature and strength of these minerals has already been pointed out (Spray, 1992). At higher temperatures, the strength of the silicates will decrease, but so also will the thermal energy required to melt that phase. There is a tendency for quartzo-feldspathic minerals to lie slightly below the best-fit line and for mafic minerals to lie above the line, suggesting some dependence of q/h on whether the host rock is mafic or felsic. In this study, the localities examined are all quartzo-feldspathic in composition. Overall, however, the W/M ratio is not expected to be sensitive to the host rock mineral composition. The best-fit line has a slope of 0.62 ($r^2 = 0.61$) and this corresponds to $q/3h$.

For brittle processes, the wear coefficient k is expected to be between 0.1 and1 (Scholz, 1987) and natural faults appear to be characterized by high wear rates (Scholz, 1987; Power et al., 1988). Assuming a coefficient of friction of $\mu = 0.75$ and using the mean W/M ratio from the Homestake shear zone (0.58, Table 1) with $q/3h = 0.62$ (Fig. 3), Eq. (7) yields a value for k of 0.7. The ratio k/μ is, therefore, close to 1 and, for a given slip event, can be regarded as constant.

In summary, Eq. (7) indicates that the W/M ratio is independent of normal stress (and, therefore, fault depth), fault area, and displacement. In addition, the data in Fig. 3 indicate it is also independent of the mineralogy. That μ and k

Table 2
Thermal and strength properties of common silicates

Mineral	C_p[a] (J/cm^3)	T[b] (°C)	Heating interval	H_f (kJ/cm^3)	q (kJ/cm^3)	Strength[c] (MN/m^2)
Anorthite	3.2	827	200–1550	0.8	5.1	2166
Albite	3.2	827	200–1100	0.8	3.7	1666
Orthoclase	3.2	827	200–1150	0.8	3.8	1666
Quartz	3.1	827	200–1730	0.8	5.5	2800
Fayalite	4.2	827	200–1590	2.0	7.8	2160–2800
Diopside	3.8	827	200–1400	1.2	5.7	1500–1267
Tremolite	3.4	427	200–850	1.2	3.4	1133–1666
Muscovite	3.3	427	200–650	1.2	2.7	333–666

[a] See Robie et al. (1978).
[b] Temperature at which heat capacity was chosen.
[c] See Spray (1992).

may vary under certain conditions cannot at present be ruled out and this represents a possible limitation of the analysis.

5.4. Transient wear/melt ratios

Given that seismic slip is a transient phenomenon and that transient wear appears to characterize natural faults better than steady-state wear (Power et al., 1988), an alternative approach is to take the ratio of the transient wear and melt equations presented above. It is interesting to note that Eqs. (2) and (6) have the same functional form. Eq. (2) is based on the assumption that the wear rate is related to the initial fault roughness and Eq. (6) is based on the assumption that the shear stress on the fault decreases as melt volume increases. Eq. (2) indicates that the volume of wear rapidly approaches v_0 ($= 2Ar$) after a few centimeters of displacement, and this represents the initial volume of material by which the fault deviates from a flat surface. Eq. (6) indicates that the melt volume also rapidly approaches V ($= At$), the fault volume, so that the ratio of Eqs. (2) and (6) approaches *2r/t* after a few centimeters of displacement.This represents the ratio of initial fault roughness to fault thickness. Because r is the distance by which the fault deviates from a flat surface, a maximum value of r is *t/2,* so that a maximum value of *2r/t* is 1:

$$W/M = <1 \tag{8}$$

This is consistent with the measured *W/M* ratios (Fig. 2) and also with those cited in the literature.

6. A geothermometer based on thermodynamic efficiency

Because of the high strain rates involved, seismic rupture appears to be essentially adiabatic (Spray, 1992). Heat will diffuse away from the fault for a distance given by $(kt)^{0.5}$ where k is thermal diffusivity ($\approx 10^{-6}$ m^2/s) and t is time. In order for the heat to be confined to 10^{-3} m or less of the fault surface, the heat generation (and a displacement of say 0.1 m) must occur in one second or less. Thus, adiabatic conditions only occur for slip velocities faster than about 0.1 m/s, which is below typical seismic velocities of 1 m/s.

During seismic faulting, some energy is dissipated as frictional heat. The remainder of the energy is expended on either seismic wave radiation, work against gravity or work on frictional wear processes (Husseini, 1977; Kanamori, 1994). Work against gravity will be negligible for a pure strike-slip fault and is probably small for low-angle thrust faults. For moderate and large earthquakes in southern California, the seismic energy was only 10^{-3} times the seismic moment (Fig. 9 in Kanamori (1994)). In a case where extensive melting likely occurred during a large earthquake, the seismic radiation energy was only 10^{-2} times the energy dissipated as heat (Kanamori et al., 1998). The assumption is made here that radiated seismic energy and gravitational energy are, therefore, negligible compared with frictional processes. The more frictional heat generated, the more melt produced, and conversely, the more energy expended on fracturing and grain size reduction, the more wear material produced. The *W/M* ratio is, therefore, interpreted as reflecting the conversion of mechanical work to heat. The efficiency of this conversion is treated by classical thermodynamics.

By the First Law (conservation of energy), $dE = dq + dw$, where q is heat, E is internal energy and w is work done by the system. Under adiabatic conditions $dq = 0$ and, therefore, $dE = dw$. This latter equality indicates that, because no heat can enter or leave the system, the increase in internal energy must equal the work done and that these two quantities cannot vary independently. This places important constraints on the behavior of the system. Assuming ideal behavior, the thermal work done in faulting produces a change in internal energy (and temperature) such that $dE = C_v dT$ where C_v is the heat capacity at constant volume and dT is the change in temperature (Dickerson, 1969). If melting occurs, $C_v dT$ is replaced by $C_v dT + H_f$, which is the heat (q) required for this melting. The mechanical work done of interest here is solely the work done in producing gouge (w_{wear}) and we exclude other energy sinks such as radiated seismic energy and work against gravity. Equating dE ($= q$) and w_{wear} and re-arranging:

$$w_{wear}/q < 1 \tag{9}$$

The left side of this equation represents the ratio of mechanical to thermal energy. The inequality reflects the fact that frictional melting is an irreversible process, and irreversible processes do less useful work than reversible ones, or conversely, they produce more heat (Lewis and Randall, 1961). As pointed out above, the *W/M* ratio is interpreted as a proxy for the left hand side of Eq. (9) so that:

$$W/M = w_{wear}/q < 1. \tag{10}$$

Some confusion may arise between Eq. (7) and Eq. (10) as they both contain heat and work energy terms. In Eq. (7), these refer to the thermal energy necessary to melt the asperities and the mechanical strength of the asperities, respectively. Because the strength of the asperities varies with melting temperature (Fig. 3), the *W/M* ratio in Eq. (7) is independent of these rock properties. In Eq. (10), *W/M* is inversely proportional to q,where q in this case is the energy partitioned by the fault into thermal energy. *W/M* is proportional to w_{wear}, where w_{wear} is the energy partitioned into mechanical work. Eq. (7) refers, therefore, to the fault mechanical and thermal properties, whereas Eq. (10) refers to energy partitioning during faulting, which is a parameter related to thermodynamic efficiency.

Adiabatic frictional melting can be regarded as a heat engine (Fig. 4a) in reverse, operating between two temperature reservoirs, in which work is converted to heat (Fig. 4b). The fault does work on its surroundings at ambient temperature (cold reservoir) and heat is generated to produce a frictional melt (hot reservoir). The efficiency of the process

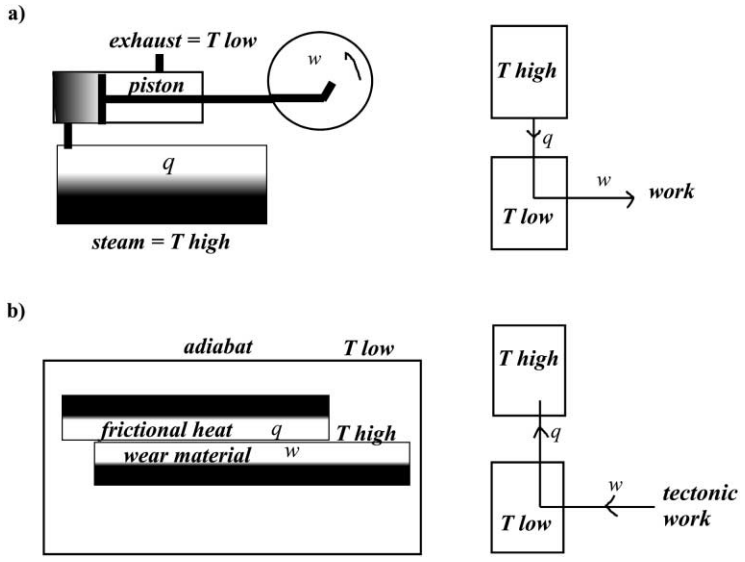

Fig. 4. (a) A steam engine as an example of a heat engine operating between two temperatures whereby heat from the hot reservoir (steam) is converted to mechanical work and waste heat is emitted to the exhaust at the lower temperature. The efficiency of the conversion of heat to work is given by $w/q = (T_{high} - T_{low})/T_{high}$. The efficiency is <1 and can only approach 100% in the case of an infinitely hot reservoir or a cold reservoir at absolute zero. (b) A rapidly slipping fault can be regarded as an adiabatic heat engine in reverse (i.e. a heat pump) in which the fault does mechanical work at the ambient country rock temperature and produces a frictional melt at a higher temperature. The ratio of thermal to mechanical work is given by $q/w = T_{high}/(T_{high} - T_{low})$. As T_{low} approaches T_{high}, the process becomes more efficient and more thermal energy is evolved. See also Fig. 6.

is defined as (Lewis and Randall, 1961):

$$w_{wear}/q = (T_{high} - T_{low})/T_{high} \quad (11)$$

where T_{high} refers to the hot reservoir, T_{low} to the cold reservoir (in degrees Kelvin), and w_{wear} and q refer to wear energy and heat energy, respectively. This applies only to a reversible process, but real processes will approach it in the limiting case. Since T_{low} can never reach absolute zero, Eqs. (9) and (11) are consistent with each other. Combining Eqs. (10) and (11):

$$W/M = (T_{high} - T_{low})/T_{high} \quad (12)$$

If T_{high} is assumed or known and *W/M* is measured, an estimate of T_{low} can be simply made. Conversely, if the country rock temperature is known, the melt temperature can be calculated.

6.1. Application of the geothermometer

Fig. 5 is a plot of Eq. (12) for various ambient temperatures (T_{low}) and melting temperatures (T_{high}), contoured for different *W/M* values (heavy lines). The wear/melt ratios measured in this study are plotted on this diagram. Excluding the eclogite facies pseudotachylytes temporarily, these values indicate ambient country rock temperatures of 123–387°C, assuming a melting temperature of 927°C. From Fig. 5 it clear, however, that the estimate of the country rock temperature is not particularly sensitive to the assumed melting temperature (T_{high}), especially for higher *W/M* ratios (see below).

The estimated range of country rock temperatures correspond to depths of 5–15.5 km (assuming a geotherm of 25°C/km), which is consistent with the current idea that frictional melting dominates the brittle regime in the upper crust (e.g. Snoke and Tullis, 1998). Although none of the *W/M* ratios were measured on samples displaying a mylonitic overprint, pseudotachylytes at both Fort Foster (Swanson, 1988) and South mountain (Fig. 1b; Goodwin et al., 1998) have been overprinted by greenschist grade mylonitic textures, suggesting some melts formed close to or below the brittle-plastic transition in the crust (about 350°C, O'Hara et al., 1997). The Homestake shear zone (Colorado) and the Nason terrane pseudotachylytes (Washington) do not show this overprinting, indicating they formed below about 350°C, broadly consistent with the results in Table 1.

In the case of ultradeep pseudotachylytes from western Norway, garnet-pyroxene geothermometry indicates a melt temperature of 790–920°C, and an ambient country rock temperature corresponding to eclogite facies (670°C; Austrheim et al., 1996). Samples indicate wear/melt ratios of 0.09–0.17 (Table 1), and using a melt temperature of 927°C, the same as at other locations for the purposes of comparison, host rock temperatures of 723–819°C are indicated (Table 1). These values are somewhat higher than the independent estimate of 670°C, but nevertheless indicate very high country rock temperatures by comparison with the other localities. Using a lower melt temperature of 800°C yields a mean temperature of 658°C in good agreement with the 670°C estimate for eclogite conditions (Table 1). In general, the metamorphic grade of the host rocks at the localities studied places a maximum value on the ambient host rock temperature at the time of melting and the

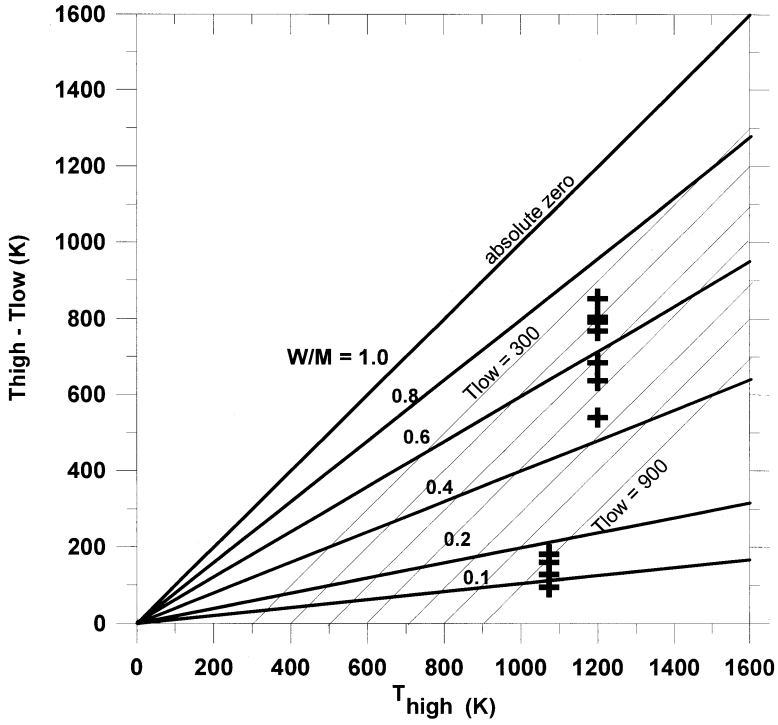

Fig. 5. Plot of Eq. (11) for different values of T_{low} (ambient country rock temperature) and for different wear/melt ratios (heavy lines). The crosses indicate wear/melt ratios measured in this study. Ambient crustal temperatures (T_{crust}) and assumed melt temperatures (T_{melt}) are given in Table 1 (in degrees Celsius).

temperatures estimated here are consistent with this constraint (Table 1).

6.2. Error estimates

Based on the 2σ error bars on measured *W/M* ratios (Fig. 2), the error on the estimated ambient country rock temperature is about ± 70°C (Fig. 5). From Fig. 5 it is also clear that as the *W/M* ratio increases, its slope comes closer to that of the T_{low} isotherms, so that the assumed temperature of the melt becomes less important. For example, the Homestake shear zone *W/M* value of 0.64 (Table 1) corresponds to an ambient country rock temperature of 159°C, assuming a melt temperature of 927°C, but increases by only 72° for a melt temperature of 1127°C.

The validity of applying equilibrium thermodynamics to a highly irreversible process such as frictional melting may be an additional source of error. Equilibrium thermodynamics can be usefully applied, however, to irreversible systems if the system can be broken down into subsystems large enough to have macroscopic properties, but small enough so that large gradients do not exist (Lewis and Randall, 1961). In the present context, this refers to clast concentration gradients rather than chemical gradients. On the scale of a thin section, the distribution of clast material is commonly homogeneous (e.g. Fig. 1a) so that measurements at this scale appear to represent an equilibrium state. High-power optical microscopy is the preferred method, which allows coverage of an entire thin section and also resolves the smallest clast sizes.

Of the various clast-melt geometries illustrated in the literature (e.g. Fig. 2 in Sibson (1975)), the method outlined here should only be applied to fault-generated melts in which the clasts in the melt can be reasonably interpreted as having being derived from the walls during a single frictional melting event. Other examples commonly represent either injection of melt into pre-existing breccia or vein networks, giving rise to very high apparent clast/matrix ratios. These situations cannot be regarded as adiabatic because the melt has traveled some distance from the source; in addition the clasts need not be contemporaneous with the same event that produced the melt. Such samples should be avoided in applying the current technique.

It is encouraging that the four samples numbered 41.5 through 41.15 in the Homestake shear zone, which come from the same outcrop, yield an internally consistent temperature range of 135–59°C (Table 1). In addition, the agreement of the independent country rock temperature estimate for the eclogite-facies pseudotachylytes (670°C, based on Fe/Mg exchange between garnet and pyroxene) with the mean estimate of four samples here (658°C) is also evidence that equilibrium thermodynamics can be usefully applied to these rocks (O'Hara and Boundy, 2000).

7. Discussion

In general, the conversion of work to heat is an irreversible process and the temperature at which the conversion takes place is a measure of the efficiency of

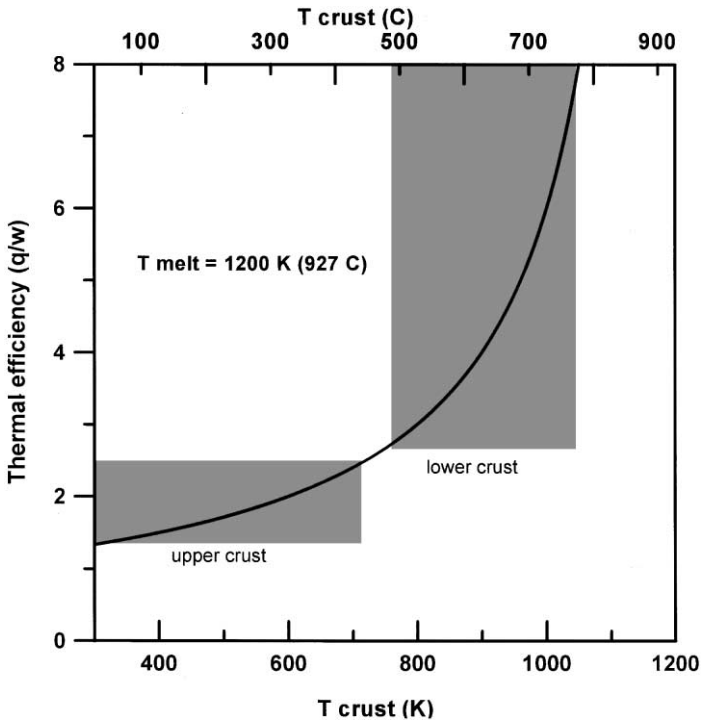

Fig. 6. Plot of the expression for maximum thermal efficiency, $q/w = T_{high}/(T_{high} - T_{low})$, where T_{high} is the assumed melt temperature, T_{low} is the ambient crustal temperature and q/w is the ratio of thermal to mechanical work. The assumed value for T_{high} is 1200 K (927°C). Maximum thermal efficiency in the lower crust is between approximately 300 and 800%, whereas in the upper crust it ranges between approximately 150 and 250%, so that frictional melting should be less common in the upper crust. In situations where high shear stresses can be generated in the lower crust, frictional melting can be expected to be common. Decreasing efficiencies at lower temperatures are caused by increased entropy production. Actual efficiencies for irreversible processes are substantially less.

the conversion. If an independent estimate of efficiency can be made, then the temperature of the process can be estimated. This is the basis of the proposed geothermometer.

The paucity of pseudotachylytes in the geologic record is somewhat surprising given the expectation that frictional melting should be common on exhumed faults (e.g. McKenzie and Brune, 1972). Previous studies, however, have not considered the efficiency of the melting process. The inverse of Eq. (11), $q/w = T_{high}/(T_{high} - T_{low})$, gives the maximum possible ratio of heat to work involved in the melting process, assuming the process is reversible. Fig. 6 is a plot of this expression for a melt temperature T_{high} of 927°C and a range of crustal temperatures T_{low}. The thermal efficiency decreases rapidly at shallower levels in the crust, indicating that, from a thermodynamic point of view, frictional melting should be more common at deeper levels for a given amount of work expended. For example, in the range 500–800°C in the crust, the efficiency is approximately 300–800%. At temperatures above about 300°C, however, frictional stress decreases because of the onset of rock plasticity so that frictional work should decrease. Alternatively, in the range 0–400°C, the maximum efficiency is only 150–250%. Although these efficiencies seem high, they are maximum values based on the assumption of reversible melting. Frictional melting is highly irreversible and actual efficiencies will be substantially less. Frictional melting should, therefore, be rare in the upper crust because of the relative inefficiency of the process, but also rare in the lower crust because of the onset of rock ductility. The ultra-deep frictional melts from Norway are unusual in this regard and appear to be the product of deep-focus earthquakes produced during eclogitization (Austrheim and Boundy, 1994).

It is argued that the *W/M* ratio in pseudotachylytes reflects the ratio of mechanical work to thermal work and that it is independent of several geologic variables, including displacement, stress, fault area and mineralogy. It might be argued that there are several other variables, in addition to efficiency, that are likely to affect this ratio.

For example, high temperature frictional melts might be expected to have lower *W/M* ratios compared with low temperature melts on account of increased assimilation of clasts by the hotter melt. Under adiabatic conditions, however, the hotter melt can only be produced by an equivalent increase of mechanical work done in producing wear material, so that hotter melts will also have a higher concentration of clasts, which on assimilation, produce the same *W/M* ratio as the colder melt. Under adiabatic conditions, mechanical work and thermal work cannot vary independently (i.e. $q = w$). So, it would not be fortuitous if hotter melts had a greater proportion of clasts to precisely maintain

the same *W/M* ratio—this situation is required by the principle of conservation of energy.

It might also be argued that hydrous minerals would be expected to lower the melting temperature of the host rock minerals by providing dehydration water, resulting in more melt (and a lower *W/M* ratio) compared with a dry system. In addition to lowering the melting temperature, however, water also has the effect of lowering the strength of asperities by either stress corrosion under brittle conditions or hydrolytic weakening under plastic conditions (Scholz, 1990). This will result in more wear material, so that the ratio of thermal energy to strength (*q/h*) remains the same. The essential point concerning these objections (and other similar arguments) is that thermal and mechanical work *cannot* vary independently under adiabatic conditions; this is a consequence of the First Law. It is proposed that the only variable on which this ratio depends is the efficiency of the conversion process and this depends solely on temperature. Much additional work, however, is required before this proposition can be fully evaluated. Future work will focus on the internal consistency of the geothermometer at individual sites and also on those localities that have independent temperature estimates.

8. Conclusions

Consideration of mechanical/thermal models indicates the wear/melt ratio is independent of fault displacement, fault area, stress and host rock mineralogy, and thermodynamic arguments indicate it should also be independent of the presence or absence of water. Transient models indicate the wear/melt ratio equals $2r/t < 1$ where r is fault roughness and t is fault thickness. The wear/melt ratio is interpreted as reflecting the thermodynamic efficiency of the conversion of work to heat and depends only on the temperature of the conversion. If the melting temperature is assumed and the wear/melt ratio is measured, an estimate of the ambient crustal temperature can be made. Measurements from five localities give estimates of crustal melting in agreement with geologic evidence and current rheological models of the crust. The paucity of pseudotachylytes in the geologic record may reflect the thermodynamic inefficiency of the conversion of work to heat at low crustal temperatures. Finally, some of the ideas presented here may provide additional insight into the energy budget, wear mechanisms, and melting processes during co-seismic slip.

Acknowledgements

I thank J. Magloughlin, J. Reynolds and M. Swanson for guidance in their respective field areas and J. Allen, D. Moecher, J. Reynolds and T. Boundy for providing samples. Thanks to E. Anderson who measured clast concentrations and J. McHugh who made excellent thin sections. An earlier version of this manuscript benefited from constructive reviews by J. Spray and D. Curewitz, which are appreciated. Journal reviews by T. Blenkinsop, R. Sibson and W. Power substantially improved the manuscript. This study would not have been possible without the support of NSF grants EAR-9814851 and EAR-9507982 for which I am grateful.

References

Allen, J.L., 1994. Fault-generated pseudotachylyte in a brittley re-activated shear zone, northeastern Sawatch Range, Colorado. Geological Society of America Abstract 29, 269.

Archard, J.F., 1953. Contact and rubbing of flat surfaces. Journal of Applied Physics 24, 981–988.

Austrheim, H., Boundy, T.M., 1994. Pseudotachylytes generated during seismic faulting and eclogitization of the deep crust. Science 265, 82–83.

Austrheim, H., Erambert, M., Boundy, T.M., 1996. Garnets recording deep crustal earthquakes. Earth and Planetary Science Letters 139, 223–238.

Boundy, T.M., Austrheim, H., 1998. Deep crustal eclogite-facies pseudotachylytes. In: Snoke, A.W., Tullis, J., Todd, V.R. (Eds.). Fault-related rocks—a photographic atlas. Princeton, New Jersey, p. 126.

Dickerson, R.E., 1969. Molecular Thermodynamics. Benjamin Inc., California.

Goodwin, L.B., Ferranti, C.J., 1994. Pseudotachylyte in a metamorphic core complex: Frictional melting facilitated by a hydrous mafic phase. Geological Society of America Abstract 26, 269.

Goodwin, L.B., Reynolds, S.J., Ferranti, C.J., Ellzey, P.D., Lister, G.S., 1998. Pseudotachylytes from a metamorphic core complex. In: Snoke, A.W., Tullis, J., Todd, V.R. (Eds.). Fault-related rocks—a photographic atlas. Princeton, New Jersey, p. 124.

Hobbs, B.E., Ord, A., Teyssier, C., 1986. Earthqakes in the ductile regime? Pure and Applied Geophysics 124, 309–336.

Husseini, M.I., 1977. Energy balance for the motion along a fault. Geophysical Journal of the Royal Astronomical Society 49, 699–714.

Kanamori, H., 1994. Mechanics of earthquakes. Annual Review of Earth and Planetary Science Letters 22, 207–237.

Kanamori, H., Anderson, D.L., Heaton, T.H., 1998. Frictional melting during the rupture of the 1994 Bolivian earthquake. Science 279, 839–841.

Lewis, G.N., Randall, M., 1961. Thermodynamics. 2nd ed. McGraw-Hill, New York (revised by Pitzer, K.S., Brewer, L.).

Logan, J.M., Teufel, L.W., 1986. The effect of normal stress on the real area of contact during frictional sliding in rocks. Pure and Applied Geophysics 124, 471–486.

Maddock, R.H., 1992. Effects of lithology, cataclasis and melting on the composition of fault-generated pseudotachylytes in Lewisian gneiss, Scotland. Tectonophysics 204, 261–278.

Magloughlin, J.F., 1989. The nature and significance of pseudotachylyte from the Nason terrane, North Cascade Mountains, Washington. Journal of Structural Geology 11, 907–917.

Magloughlin, J.F., 1992. Microstructural and chemical changes associated with cataclasis and frictional melting at shallow crustal levels: the cataclasite–pseudotachylyte connection. Tectonophysics 204, 243–260.

Magloughlin, J.F., 1998. Amygdules within pseudotachylyte. In: Snoke, A.W., Tullis, J., Todd, V.R. (Eds.), Fault-related rocks—a photographic atlas. Princeton, New Jersey, p. 88.

McKenzie, D., Brune, J.N., 1972. Melting on fault planes during large earthquakes. Geophysical Journal of the Royal Astronomical Society 29, 65–78.

Moecher, D.P., Cleary, M., O'Hara, K.D., Allen, J.L., 1999. Mineralogy of a mullite-bearing pseudotachylyte. Geological Society of America Abstracts 31, 359.

O'Hara, K.D., Boundy, T.M., 2000. Application of a new geothermometer

to frictional melting in the crust. Geological Society of America Abstracts 32, 99.

O'Hara, K.D., Sharp, Z.D., 2001. Chemical and oxygen isotope composition of natural and artificial pseudotachylytes: the role of water in frictional fusion. Earth and Planetary Science Letters 184, 393–406.

O'Hara, K.D., Sharp, Z.D., Moecher, D.P., Jenkin, G.R.T., 1997. The effect of deformation on oxygen isotope exchange in quartz and feldspar and the significance of isotopic temperatures in mylonites. Journal of Geology 105, 193–204.

Power, W., Tullis, T.E., Weeks, J.D., 1988. Roughness and wear during brittle faulting. Journal of Geophysical Research B12, 15,268–15,278.

Ray, K.S., 1999. Transformation of cataclastically deformed rocks to pseudotachylyte by pervasion of frictional melt: inferences from clast-size analysis. Tectonophysics 301, 283–304.

Reynolds, S.J., Lister, G.S., 1987. In: Davis, G.H., Vanden Dolder, E.M. (Eds.). Field Guide to the Lower and Upper Plate Rocks of the South Mountains Detachment, Arizona, pp. 244–248. Geological Society of America, 100th Annual Meeting.

Robie, R.A., Hemingway, B.S., Fisher, J.R., 1978. Thermodynamic properties of minerals and related substances at 298.15 K and 1 bar pressure (10^5 Pascals) and at higher temperatures. United States Geological Survey Bulletin 1452.

Scholz, C.H., 1987. Wear and gouge formation in brittle faulting. Geology 15, 493–495.

Scholz, C.H., 1990. The mechanics of earthquakes and faulting. Cambridge Press, New York.

Shimamoto, T., Nagahama, H., 1992. An argument against the crush origin of pseudotachylytes based on the analysis of clast-size distribution. Journal of Structural Geology 14, 999–1006.

Sibson, R.H., 1975. Generation of pseudotachylte by ancient seismic faulting. Geophysical Journal of Royal Astronomical Society 43, 775–794.

Sibson, R.H., 1980. Transient discontinuities in ductile shear zones. Journal of Structural Geology 2, 165–171.

Snoke, A.W., Tullis, J., 1998. An overview of fault rocks. In: Snoke, A.W., Tullis, J., Todd, V.R. (Eds.). Fault-related rocks—a photographic atlas. Princeton, New Jersey, pp. 3–18.

Spray, J.G., 1992. A physical basis for the frictional melting of some rock forming minerals. Tectonophysics 204, 205–221.

Spray, J.G., 1993. Viscosity determinations of some frictionally generated silicate melts: implications for fault zone rheology at high strain rates. Journal of Geophysical Research B5, 8053–8068.

Spray, J.G., 1995. Pseudotachylyte controversy: fact or friction. Geology 23, 1119–1122.

Swanson, M.T., 1988. Pseudotachylyte-bearing strike-slip duplex structures in the Fort Forster brittle zone, S. Maine. Journal of Structural Geology 10, 813–828.

Swanson, M.T., 1992. Fault structure, wear mechanisms and rupture processes in pseudotachylyte generation. Tectonophysics 204, 223–242.

Techmer, K.S., Ahrendt, H., Weber, K., 1992. The development of pseudotachylyte in the Ivrea–Verbano zone of the Italian Alps. Tectonophysics 204, 307–322.

Tsutsumi, A., 1999. Size distribution of clasts in experimentally produced pseudotachylytes. Journal of Structural Geology 21, 305–312.

Wang, W., Scholz, C.H., 1994. Wear processes during frictional sliding of rock: a theoretical and experimental study. Journal of Geophysical Research B4, 6789–6799.